

 Open Access Full Text Article

ORIGINAL RESEARCH

# Anti-MRSA malleable liposomes carrying chloramphenicol for ameliorating hair follicle targeting

Ching-Yun Hsu<sup>1,2,\*</sup>Shih-Chun Yang<sup>3,4,\*</sup>Calvin T Sung<sup>5</sup>Yi-Han Weng<sup>4</sup>Jia-You Fang<sup>2,4,6,7</sup>

<sup>1</sup>Department of Nutrition and Health Sciences, <sup>2</sup>Research Center for Food and Cosmetic Safety and Research Center for Chinese Herbal Medicine, Chang Gung University of Science and Technology, Kweishan, <sup>3</sup>Department of Cosmetic Science, Providence University, Taichung, <sup>4</sup>Pharmaceutics Laboratory, Graduate Institute of Natural Products, Chang Gung University, Kweishan, Taiwan; <sup>5</sup>School of Medicine, University of California, Riverside, CA, USA; <sup>6</sup>Chinese Herbal Medicine Research Team, Healthy Aging Research Center, Chang Gung University, <sup>7</sup>Department of Anesthesiology, Chang Gung Memorial Hospital, Kweishan, Taiwan

\*These authors contributed equally to this work

**Abstract:** Pathogens usually invade hair follicles when skin infection occurs. The accumulated bacteria in follicles are difficult to eradicate. The present study aimed to assess the cutaneous and follicular delivery of chloramphenicol (Cm)-loaded liposomes and the antibacterial activity of these liposomes against methicillin-resistant *Staphylococcus aureus* (MRSA). Skin permeation was conducted by in vitro Franz diffusion cell. The anti-MRSA potential was checked using minimum inhibitory concentration (MIC), minimum bactericidal concentration (MBC), a well diffusion test, and intracellular MRSA killing. The classic, dimyristoylphosphatidylcholine (DMPC), and deoxycholic acid (DA) liposomes had a vesicle size of 98, 132, and 239 nm, respectively. The incorporation of DMPC or DA into the liposomes increased the bilayer fluidity. The malleable vesicles containing DMPC and DA showed increased follicular Cm uptake over the control solution by 1.5- and 2-fold, respectively. The MIC and MBC of DA liposomes loaded with Cm were 62.5 and 62.5–125 µg/mL, comparable to free Cm. An inhibition zone about 2-fold higher was achieved by DA liposomes as compared to the free control at a Cm dose of 0.5 mg/mL. DA liposomes also augmented antibacterial activity on keratinocyte-infected MRSA. The deformable liposomes had good biocompatibility against keratinocytes and neutrophils (viability >80%). In vivo administration demonstrated that DA liposomes caused negligible toxicity on the skin, based on physiological examination and histology. These data suggest the potential application of malleable liposomes for follicular targeting and the treatment of MRSA-infected dermatologic conditions.

**Keywords:** chloramphenicol, malleable liposomes, deoxycholic acid, hair follicle, MRSA, antibacterial activity

## Introduction

Bacterial infections are becoming increasingly serious health problems. Among these, *Staphylococcus aureus* has emerged as a leading infectious bacterium strain, especially for superficial and invasive skin infection.<sup>1</sup> The substantial challenge in *S. aureus* infection management is antibiotic resistance, as demonstrated by the methicillin-resistant *S. aureus* (MRSA). Resistance to methicillin is found in >60% of *S. aureus*, the most prevalent bacteria in cutaneous infection.<sup>2</sup> Topically applied antibacterial chemotherapy is fundamental in the treatment of skin infection. The use of nanoparticles as the carriers of antibacterial agents represents a novel strategy to overcome drug-resistant strains in skin. The unique features of nanoparticles, such as controllable size, high surface-area-to-mass ratio, and high reactivity to pathologic microorganisms, contribute to their advantages for antimicrobial therapy.<sup>3</sup>

Correspondence: Jia-You Fang  
Pharmaceutics Laboratory, Graduate Institute of Natural Products, Chang Gung University, 259 Wen-Hwa 1st Road, Kweishan, Taoyuan 333, Taiwan  
Tel +886 3 211 8800  
Fax +886 3 211 8236  
Email fajy@mail.cgu.edu.tw

Approximately 25% of cutaneous bacteria accumulate within the hair follicles.<sup>4</sup> *S. aureus* violation in the follicles causes folliculitis, furuncle, and hidradenitis suppurativa.<sup>5,6</sup> An ideal antimicrobial treatment would be efficiently delivered to the infection area and targeted to the bacteria. The nanoparticles provide a means to specifically transfer the drugs into cutaneous appendages.<sup>7</sup> Liposomes, functioning as nanocarriers with a phospholipid bilayer membrane, have been demonstrated to be useful for follicular targeting.<sup>8,9</sup> Liposomes possess some beneficial effects such as good biocompatibility, sustained drug release, and improved bioavailability. The delivery and therapeutic potential of the drugs can be controlled by modulating liposomal compositions and properties. The incorporation of ethanol or edge activators into liposomes can increase deformability, producing malleable vesicles. The soft and flexible structure of malleable liposomes can enhance cutaneous permeation through their ability to squeeze through intercellular spaces.<sup>10</sup> Treating *S. aureus* invasion by follicular delivery of malleable liposomes is conceivable, although studies related to this possibility are currently lacking. The aim of the present research was to prepare and assess malleable liposomes for improved follicular transport and anti-MRSA activity.

Chloramphenicol (Cm) was employed as the model drug. Previous study<sup>11</sup> has indicated an antagonist effect on antimicrobial activity of combined Cm and silver nanoparticles, suggesting the importance of selecting feasible nanosystems for Cm. To enhance cutaneous permeation and follicular targeting of Cm, we added dimyristoylphosphatidylcholine (DMPC) or deoxycholic acid (DA) to liposomes, in order to produce flexible vesicles. The ability of DMPC and DA to elasticize liposomes has been previously shown.<sup>12,13</sup> The physicochemical properties of the liposomes were evaluated with regard to Cm skin penetration and anti-MRSA effect. *S. aureus* is difficult to kill using conventional antibiotics because of its intracellular persistence in host cells.<sup>14</sup> The antimicrobial efficacy of the liposomes was also investigated using MRSA-infected keratinocytes.

## Materials and methods

### Preparation of liposomes

Soybean phosphatidylcholine (SPC, Phospholipon® [American Lecithin Company, Oxford, CT, USA] 80H, 2.5%) and cholesterol (0.7%) were dissolved in 5 mL of a chloroform/ethanol (2:1) solution. DMPC (1%) or DA (0.15%) was added to the solution if necessary. The solvent was evaporated in a rotary evaporator at 50°C, and solvent traces were

removed under vacuum overnight. The phospholipid film was hydrated with double-distilled water containing Cm using a probe-type sonicator at 35 W for 30 minutes. The Cm concentration in the final product was 4 mg/mL. The liposomal system was centrifuged at 48,000×g and 4°C for 40 minutes to withdraw the unencapsulated drug in the supernatant. The liposomes were reconstituted by adding water to the pellets to achieve a Cm concentration of 1 mg/mL.

### Vesicle diameter and zeta potential

The average diameter (z-average) and zeta potential of the prepared liposomes were measured using a laser scattering method (Nano ZS90; Malvern Instruments, Malvern, UK). The determination was performed at the liposomal concentration after a 100-fold dilution with double-distilled water. The measurement was repeated three times per sample for three batches. Nano ZS90 software version 7.11 (Malvern Instruments) was used.

### Molecular environment

The molecular environment of all vesicles was detected by fluorescence spectrophotometry (F2500; Hitachi Ltd, Tokyo, Japan) based on the solvatochromism of Nile red. The liposomes were incorporated with Nile red (1 ppm). The emission spectra of the dye-loaded liposomes were scanned from 550 to 700 nm. The excitation wavelength was set to 546 nm. A representative image from three independent measurements was shown.

### Differential scanning calorimetry (DSC)

The transition point of SPC in the liposomal suspension was measured using a Q2000 calorimeter (TA Instruments, New Castle, DE, USA). All liposomes were lyophilized before the analysis. The samples were weighed and sealed in the calorimeter. The heating curve was recorded from 20°C to 90°C at a scan rate of 10°C/min under nitrogen. The software used to calculate the enthalpy was Advantage® (TA Instruments). A representative image from three independent measurements was shown.

### Animals

Eight-week-old female nude mice (ICR-Foxn1nu) purchased from National Laboratory Animal Center (Taipei, Taiwan) were used in the in vitro skin permeation and in vivo cutaneous irritation experiments. The protocol was approved by the Institutional Animal Care and Use Committee of Chang Gung University. All animals were housed and handled according to the institutional guidelines.

## In vitro skin permeation

In vitro Cm absorption was conducted by Franz diffusion cell. The dorsal skin of a female nude mouse (8 weeks old) was mounted between the donor and receptor with the stratum corneum (SC) facing up toward the donor. The donor and receptor were filled with liposomal suspension (0.5 mL) and pH 7.4 buffer (5.5 mL), respectively. The Cm dose in the donor was 1 mg/mL. The other procedures and the drug amount extracted from the skin were the same as in our previous study.<sup>15</sup> Differential stripping and cyanoacrylate casting were employed to detect Cm uptake in the hair follicles as previously described.<sup>16</sup> The Cm content was quantified by high performance liquid chromatography (HPLC). The HPLC system was the Hitachi 2-series. A 25-cm-long C18 column (Merck Millipore, Billerica, MA, USA) was used as the stationary phase. The mobile phase used methanol and pH 2 double-distilled water adjusted by phosphoric acid (55:45). The ultraviolet wavelength detected for Cm was 280 nm.

## Minimum inhibitory concentration (MIC) and minimum bactericidal concentration (MBC)

MIC and MBC were determined to evaluate the antibacterial effect of classic, DMPC, and DA liposomes against MRSA (ATCC 33591). A 2-fold broth-dilution method was used to detect MIC. The overnight culture of MRSA was diluted in tryptic soy broth (TSB) medium to attain an optical density at 600 nm ( $OD_{600}$ ) of 0.01 (about  $2 \times 10^6$  colony forming units [CFU]/mL). The MRSA population was exposed to several dilutions of liposomes containing Cm ranging from 3.9 to 1,000  $\mu$ g/mL and incubated at 37°C for 20 hours. An enzyme-linked immunosorbent assay reader was used to detect MIC at 595 nm. MIC was recorded as the highest dilution revealing no bacterial growth. For the MBC assay, the bacteria were diluted in phosphate-buffered saline (PBS) and positioned on plates. The liposomes with different dilutions were incubated with MRSA for 20 hours at 37°C. CFU were counted. The highest dilution, which resulted in 99.9% reduction of cell numbers, was recognized as MBC.

## Disk diffusion assay

This assay was performed, based on a previous study,<sup>17</sup> by plating MRSA ( $OD_{600} = 0.8$ ) on the agar medium. MRSA grown during the mid-logarithmic phase were added to 30 mL of molten 7.5% TSB agar at 47°C. This suspension was gently mixed using agitation for 30 seconds; then, a 5-mL portion of this mixture was added onto the dish. The agar was allowed to cool until solidified. The 6-mm-diameter

disks were put on the agar surface, and liposomes containing Cm at 0.5, 1, and 2 mg/mL with a volume of 10  $\mu$ L were pipetted into the disk. The plates were incubated at 37°C for 12 hours. After this procedure, the diameter of the inhibition zone was measured. The inhibition zone size around each disk represented the mean of three axial measurements for each disk.

## Detection of MRSA death rate by flow cytometry

The viability of MRSA after liposomal treatment was examined using a Live/Dead BacLight® kit (Molecular Probes, Eugene, OR, USA). MRSA with  $OD_{600} = 0.1$  was treated with free drug or Cm-loaded liposomes (Cm concentration =200  $\mu$ g/mL) for 8 hours. The bacteria pellet was then obtained by centrifugation at 12,000 rpm for 3 minutes. The pellet was resuspended in culture medium to obtain an  $OD_{600}$  of 0.2. The aim of this process was to increase the bacterial population for facile detection by flow cytometry. After incubation at 37°C for 8 hours, the samples were stained with the kit and incubated for 15 minutes. The samples were analyzed by a flow cytometer (BD Biosciences, San Jose, CA, USA).

## Intracellular MRSA killing

Cultured human keratinocytes (HaCaT) were used as the host cells to assess the activity of liposomes toward intracellular MRSA. The HaCaT cell line was provided free by Dr Chi-Feng Hung (Fu Jen Catholic University, New Taipei City, Taiwan). This experiment was approved by the Institutional Review Board at Chang Gung University. The method was modified according to a previous study.<sup>18</sup> Briefly, keratinocytes were infected with MRSA at a multiplicity of infection (MOI) =50 for 20 minutes. MOI is the ratio of the MRSA population to the infection target cells. After being washed with PBS, the cells were incubated in 1 mL fresh medium supplemented with DA liposomes containing Cm at 31.25, 62.5, or 125  $\mu$ g/mL. After a 16-hour period, the species were rinsed with PBS. Triton X-100 (1%) was added to the cell medium to obtain the lysate.<sup>19</sup> The 1% Triton X-100 was examined using a disk diffusion test to treat MRSA for 1 hour. No inhibition zone was detected after Triton X-100 treatment, indicating that this lysis solution only damaged the mammalian cells but not the bacteria. The resultant solution was cultured on the agar dish for 20 hours and the CFU were counted. Fluorescence microscopy was employed to visualize HaCaT cells and viable MRSA. DAPI (4'-6-diamidino-2-phenylindole) and anti-*S. aureus*

antibody (Abcam, Cambridge, UK) were used to stain the keratinocyte nucleus and MRSA, respectively. The secondary antibody used in this experiment was Alexa Fluor® 488 goat anti-mouse IgG. The staining of DAPI and antibody to the mammalian cells and MRSA was performed according to a previous protocol.<sup>20</sup>

## Cytotoxicity of liposomes against keratinocytes and neutrophils

The possible cytotoxicity of liposomes on keratinocytes was determined by using the MTT method as described previously.<sup>21</sup> The cytotoxicity of neutrophils was measured by detecting lactate dehydrogenase (LDH) as demonstrated in a previous study.<sup>22</sup> The SPC concentrations in the liposomal systems for testing cytotoxicity were 0.25, 0.50, and 1.25 µg/mL.

## In vivo cutaneous irritation test

Control solution (25% ethanol in water) or DA liposomes with a volume of 0.6 mL were applied daily to the nude mouse back for 7 consecutive days with possible irritation being monitored. The application area was 1.5×1.5 cm<sup>2</sup>. After 7-day administration, the treated skin region was examined for transepidermal water loss (TEWL), skin surface pH, and erythema index (a\*). TEWL and pH were measured by Cutometer® MPA580 (Courage and Khazaka, Cologne, Germany). Erythema was analyzed using a CD100 spectroradiometer (Yokogawa, Tokyo, Japan). Hematoxylin and eosin (H&E) were utilized to stain skin slices for histological observation under optical microscopy.

## Statistical analysis

The data are presented as mean and standard deviation. The difference in the data of different experimental groups was evaluated using the Kruskal-Wallis test. The post hoc test used for checking individual differences was Dunn's test. Significance was indicated as \* for  $p<0.05$ , \*\* for  $p<0.01$ , and \*\*\* for  $p<0.001$ .

## Results

### Physicochemical properties of liposomes

Two types of soft liposomes containing DMPC and DA were prepared. Physicochemical data allowed comparison of rigid and soft liposomes as shown in Table 1. Classic liposomes were found to have a hydrodynamic size of 98 nm. Intercalation of DMPC and DA resulted in the increase of diameter to 132 and 239 nm, respectively. DA incorporation significantly increased the polydispersity index from 0.22 to 0.42. The zeta potential of the vesicles was highly negative and was not influenced by DMPC or DA loading. The negative charge corroborated the anionic nature of SPC. The encapsulation percentage for Cm was 15.0%±3.6%, 14.1%±2.0%, and 12.5%±2.3% for classic, DMPC, and DA liposomes, respectively. This loading capacity can be regarded as low since Cm is categorized as a hydrophilic drug. Free Cm from vesicles could be removed after ultracentrifugation; therefore, the completely encapsulated form was utilized throughout the experiment.

Figure 1A demonstrates the emission spectra of Nile red in liposomes. DMPC vesicles exhibited the highest fluorescence intensity, which implied that this nanosystem had the strongest lipophilicity. DA liposomes revealed weaker emission as compared to classic and DMPC liposomes, indicating a more hydrophilic nature of this deformable formulation. The crystallinity of the lyophilized liposomes was characterized using DSC (Figure 1B). For the bulk material of SPC, the melting peak was observed at 76.86°C. A DSC thermogram of classic liposomes showed an endotherm at 63.78°C, attributed to SPC melting in the vesicles. The shifted endotherm of SPC (54.14°C) and minimization of enthalpy (from 19.46 to 2.17 J/g) by DMPC intercalation were attributed to the reduced crystallinity. The peak of SPC in DA liposomes also showed a shift to the lower temperature and enthalpy (62.35°C and 6.42 J/g).

## In vitro skin permeation

The prepared liposomes were first investigated to establish skin delivery of Cm (Figure 2). Permeation experiments

**Table I** The characterization of liposomes by vesicle size, PDI, zeta potential, chloramphenicol encapsulation efficiency, and antibacterial activity

Formulation	Size (nm)	PDI	Zeta potential (mV)	MIC (µg/mL)	MBC (µg/mL)
Free drug	– <sup>a</sup>	–	–	62.5	62.5–125
Classic liposomes	97.5±12.0	0.22±0.04	-36.6±4.0	62.5–125	125–250
DMPC liposomes	132.1±43.6	0.28±0.04	-37.8±4.5	62.5–125	125–250
DA liposomes	238.5±17.1	0.42±0.09	-39.4±8.4	62.5	62.5–125

**Notes:** <sup>a</sup>Not determined. Each value represents the mean ± SD (n=3).

**Abbreviations:** MIC, minimum inhibitory concentration; MBC, minimum bactericidal concentration; PDI, polydispersity index; DA, deoxycholic acid; DMPC, dimyristoylphosphatidylcholine; SD, standard deviation.

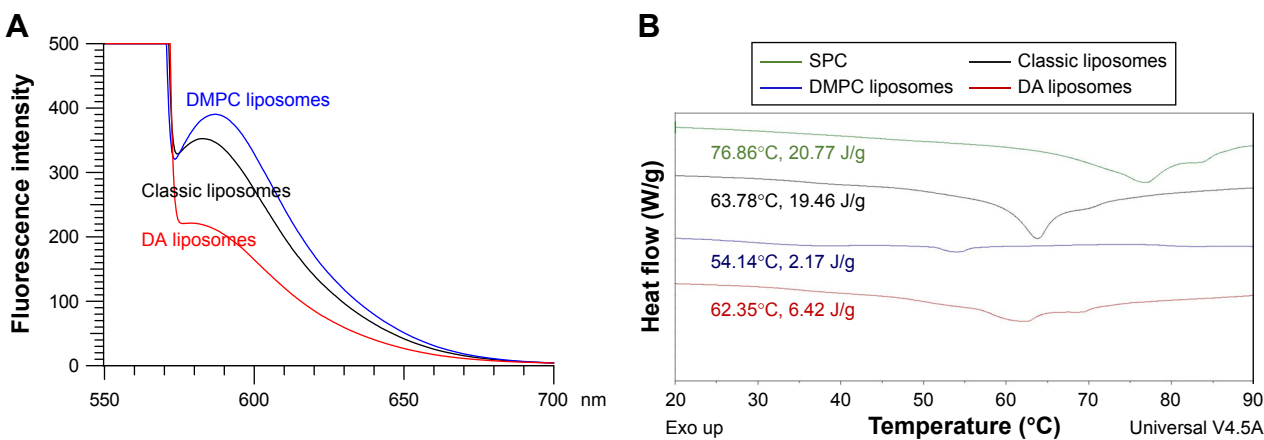


**Figure 1** Comparison of physicochemical properties of various liposomes.

**Notes:** (A) Fluorescence emission profiles of Nile red in liposomes. (B) DSC profiles of the melting process of bulk SPC and liposomes after freeze drying.

**Abbreviations:** DSC, differential scanning calorimetry; SPC, soybean phosphatidylcholine; DA, deoxycholic acid; DMPC, dimyristoylphosphatidylcholine.

conducted with nude mouse skin demonstrated a Cm skin deposition of 28 µg/g for aqueous solution and 29 µg/g for classic liposomes, with no significant difference between the groups (Figure 2A). Application with DMPC liposomes reduced skin deposition by 2-fold. The highest Cm deposition was found in DA liposomes (45 µg/g). As depicted in

Figure 2B, classic liposomes delivered less Cm to the hair follicles as compared to free Cm. Both malleable liposomes increased follicular targeting. There was a 2-fold increase in the Cm follicular level after DA liposome treatment compared to the aqueous control. The cumulative amount of Cm that penetrated across the skin was 4.4 and 4.6 µg/cm<sup>2</sup>

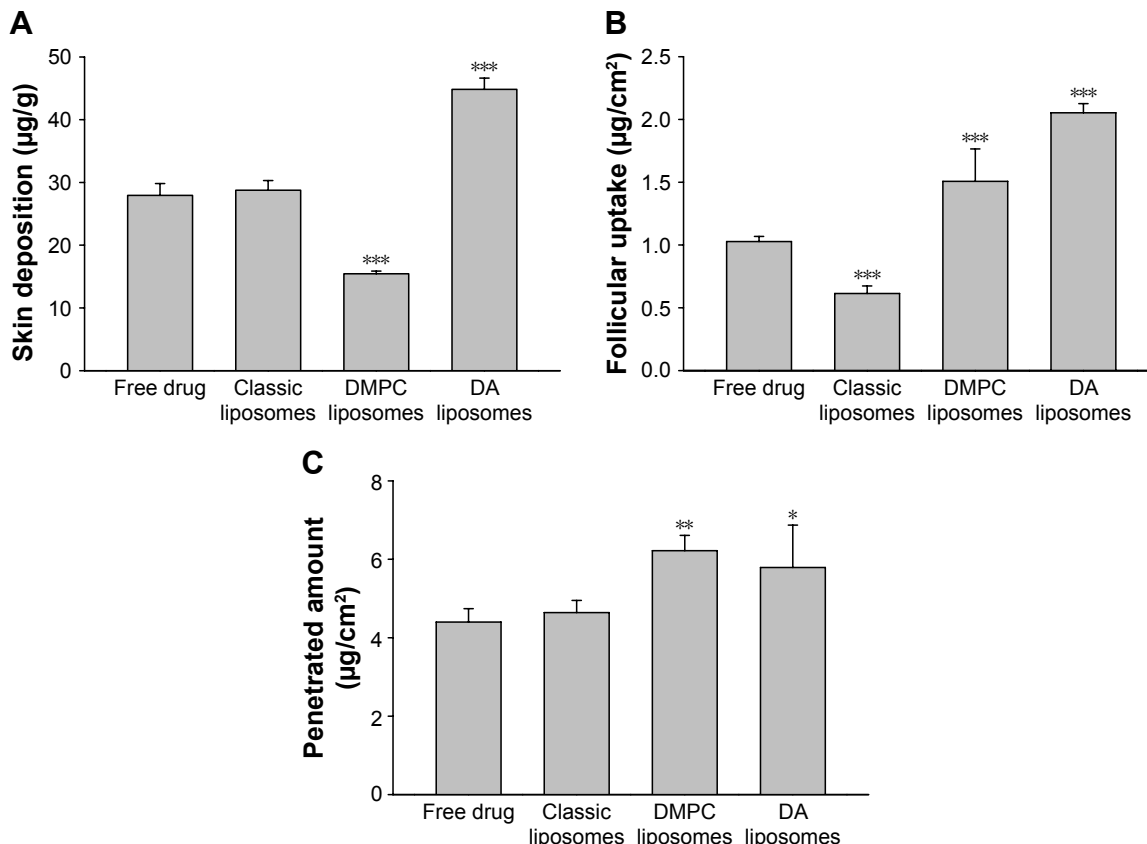


**Figure 2** In vitro skin permeation of Cm from control solution and various liposomes after 24-hour application.

**Notes:** (A) Skin deposition, (B) follicular uptake, and (C) penetrated amount in receptor. Each value represents the mean and SD (n=4). \*p<0.05, \*\*p<0.01, and \*\*\*p<0.001.

**Abbreviations:** DA, deoxycholic acid; DMPC, dimyristoylphosphatidylcholine; Cm, chloramphenicol; SD, standard deviation.

for the control group and classic liposomes, respectively (Figure 2C). The amount of penetrated Cm was higher in the case of flexible liposomes ( $6.2 \mu\text{g}/\text{cm}^2$  for DMPC liposomes and  $5.8 \mu\text{g}/\text{cm}^2$  for DA liposomes).

### Anti-MRSA activity

The liposomes were evaluated for antibacterial activity against MRSA. Table 1 summarizes the MIC and MBC values for free control and liposomes. Vehicles without Cm showed no anti-MRSA effect. The MIC and MBC for free Cm were 62.5 and  $62.5\text{--}125 \mu\text{g}/\text{mL}$ , respectively. Classic and DMPC liposomes exhibited a slightly higher MIC and MBC than the free control. Cm loading in DA liposomes maintained the same levels of MIC and MBC as free Cm. Figure 3A compares the antibacterial activity of free Cm and Cm containing liposomes judged by the inhibition zone. The inhibition diameter for free Cm at 0.5, 1, and 2 mg/mL was 0.67, 1.60, and 2.13 mm, respectively. The classic and DMPC vesicles retained the antibiotic activity of free Cm against MRSA. Higher anti-MRSA activity was noted in DA liposomes with 0.5 mg/mL Cm compared to the other vehicles. An inhibition diameter was obtained for DA liposomes about

2-fold wider than for the other liposomes. The liposomes without Cm were also examined using the disk diffusion test. We found no inhibition zone for the three nanovesicles tested. This indicated no action of the anti-MRSA effect by the liposomes in the absence of the drug. We further examined the bacterial death rate by using flow cytometry. As shown in Figure 3B, free Cm treatment induced 95% killing of MRSA. Classic and DA liposomes showed a comparable MRSA death rate compared to the control solution. The death rate of DMPC liposomes against MRSA was 73%, showing less potency than with the other formulations. Figure 3C illustrates the representative flow cytometry diagram of the live/dead strain.

MRSA is an extracellular and intracellular pathogen. Since DA nanocarriers showed the strongest anti-MRSA activity among the three liposomal formulations tested, the capability of DA liposomes to serve as a force against intracellular MRSA in infected keratinocytes was evaluated. Both free Cm and Cm-entrapped liposomes did not exert a cytotoxic effect on HaCaT cells at the concentrations tested. As shown in Figure 4A, MRSA-infected HaCaT treated by DA liposomes containing Cm exhibited a lower microbial

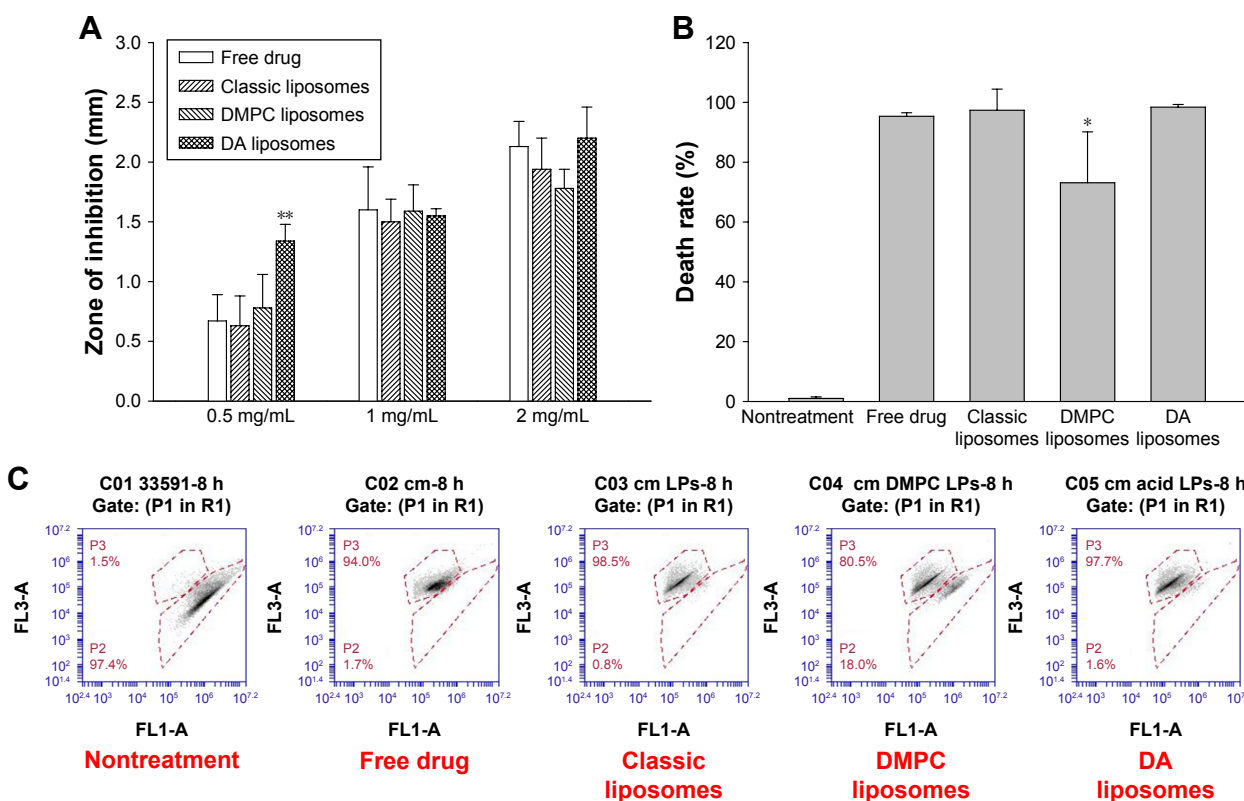


**Figure 3** Anti-MRSA activity of Cm in control solution and various liposomes.

**Notes:** (A) Zone of inhibition measured from disk diffusion assay, (B) death rate measured by flow cytometry, and (C) representative flow cytometry diagram of live/dead strain. Each value represents the mean and SD (n=3). \*p<0.05 and \*\*p<0.01.

**Abbreviations:** MRSA, methicillin-resistant *Staphylococcus aureus*; DA, deoxycholic acid; DMPC, dimyristoylphosphatidylcholine; Cm, chloramphenicol; SD, standard deviation.

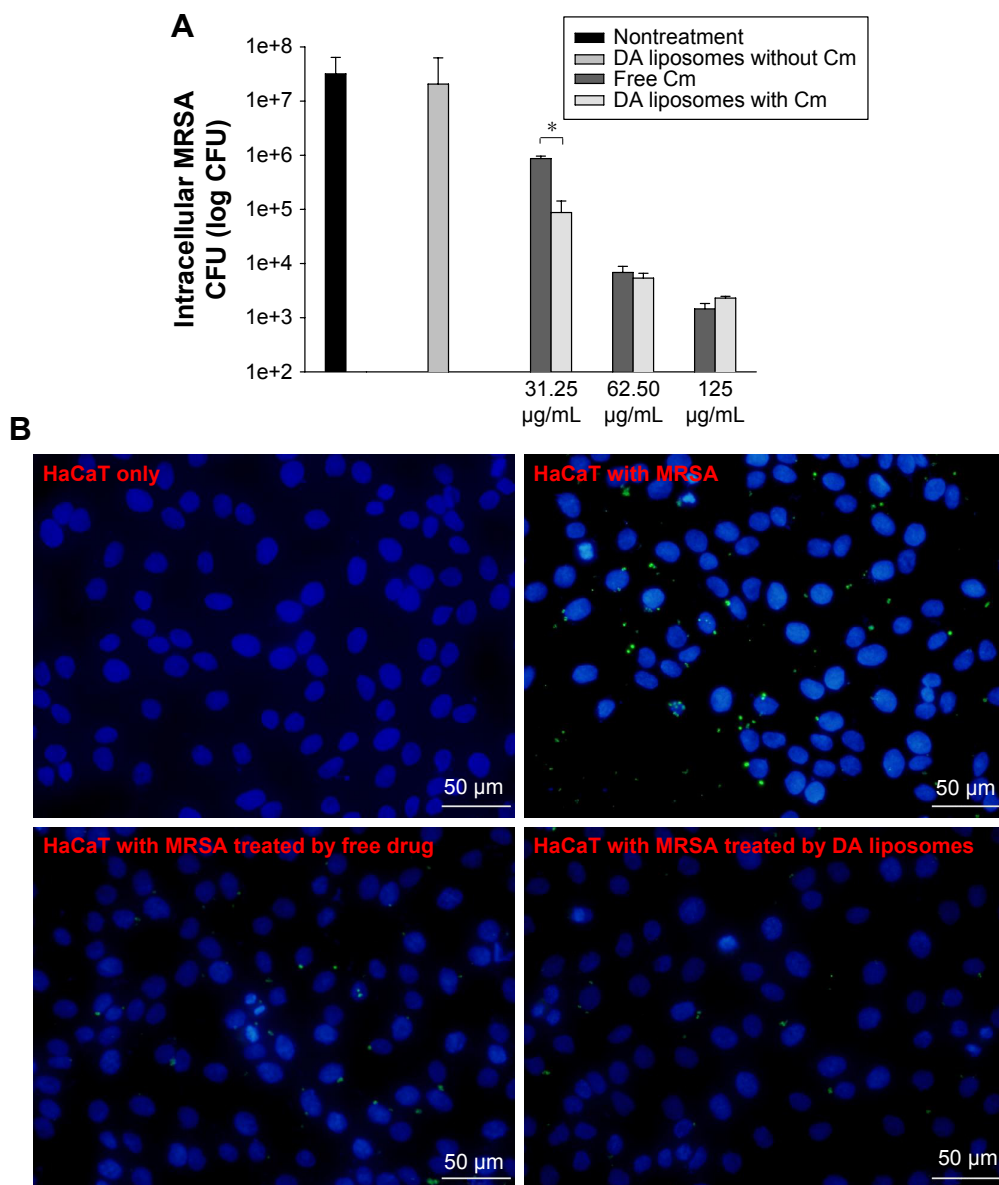


**Figure 4** Intracellular MRSA killing in keratinocytes by Cm in control solution and DA liposomes.

**Notes:** (A) Intracellular MRSA burden and (B) keratinocytes (stained by DAPI) and MRSA (stained by anti-*S. aureus* antibody) viewed by fluorescence microscopy. Each value represents the mean and SD ( $n=3$ ). \* $p<0.05$ .

**Abbreviations:** MRSA, methicillin-resistant *Staphylococcus aureus*; DA, deoxycholic acid; Cm, chloramphenicol; SD, standard deviation; DAPI, 4'-6-diamidino-2-phenylindole; CFU, colony forming units.

burden than did the free control at a lower Cm concentration (31.25 µg/mL). DA liposomes reduced the number of MRSA by 2–3 log units in comparison to nontreatment. Dose-dependent intracellular killing of MRSA was observed. There was no significant difference between the intracellular MRSA survival of free and liposomal Cm at higher concentrations. Figure 4B shows fluorescence microscopic images of MRSA incubated with keratinocytes. Green fluorescence from MRSA was visualized inside and outside HaCaT cells after incubation for 16 hours. The extracellular MRSA could be derived from the intracellular replication and the spread

from bacteria. The treatment of infected HaCaT with free and liposomal Cm at 31.25 µg/mL produced a dramatic decrease of MRSA, verifying the data obtained in Figure 4A.

### Cytotoxicity and cutaneous irritation examination

The impact of liposomes on cell viability was evaluated in two cell types, keratinocytes and neutrophils. The empty liposomes without Cm were examined in this experiment. The vesicle concentration is presented in units of SPC concentration as shown in Figure 5. SPC concentrations of 0.25,

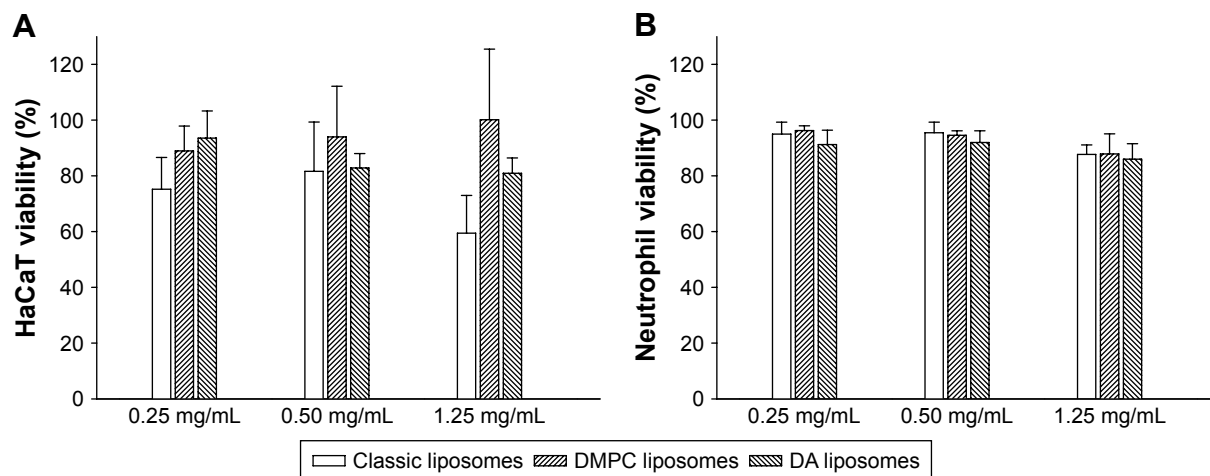


**Figure 5** Cell viability by treatment of control solution and various liposomes without Cm.

**Notes:** (A) Keratinocytes and (B) neutrophils. Each value represents the mean and SD (n=4).

**Abbreviations:** DA, deoxycholic acid; DMPC, dimyristoylphosphatidylcholine; Cm, chloramphenicol; HaCaT, keratinocytes; SD, standard deviation.

0.50, and 1.25 mg/mL used in this experiment corresponded with the Cm concentrations of 40, 80, and 200 µg/mL in liposomes, though there was no Cm in the nanovesicles in this experiment. DMPC liposomes did not have a toxic effect on HaCaT as demonstrated in the MTT assay (Figure 5A). DA liposomes without Cm showed mild cytotoxicity to HaCaT at the highest SPC concentration (1.25 mg/mL), which led to 19% less viability compared to the control. A higher magnification of cytotoxicity was observed for classic liposomes over the others, showing 59% viability at the highest concentration. Neutrophils are the predominant leukocytes in the body. The LDH assay indicates that all liposomes could maintain neutrophil viability >85% at concentrations of 0.25–1.25 µg/mL (Figure 5B). This suggests good biocompatibility of liposomes to neutrophils. The malleable liposomes showed negligible cytotoxicity at the highest SPC concentration of 1.25 mg/mL. The Cm dose in this SPC concentration in liposomes reached 200 µg/mL, which surpassed the MIC level (62.5 µg/mL) against MRSA. This result demonstrated that malleable liposomes could eradicate MRSA without affecting the viability of mammalian cells.

The change in skin physiology such as TEWL, skin surface pH, and erythema was measured by a 7-day consecutive administration of free drug and DA liposomes. TEWL is a reflection of skin barrier function. As shown in Table 2, ΔTEWL was comparable between the free control and DA liposomes. The pH values were slightly shifted to an alkaline condition. Erythema (a\*) detection indicated no skin rash in the nude mouse treated by the aqueous control and malleable liposomes. Possible skin damage was checked by H&E staining as illustrated in Figure 6. The histology

indicated no observable disruption in the intact skin that received no treatment (Figure 6A). The biopsied skin specimens after treatment of aqueous solution and DA liposomes showed comparative morphology versus the non-treated skin (Figure 6B and C). The inflammation and immune cell infiltration could be categorized as negligible.

## Discussion

Bacteria are becoming resistant even to second-line therapy as shown in the resistance of MRSA to most β-lactam antibiotics. Increasing attention has been paid to nanomedicine as an approach to efficiently treat drug-resistant microbes. In this study, we developed malleable liposomes, as they were capable of specifically delivering Cm to hair follicles for treating cutaneous pathogens. The experimental results indicated that DA liposomes showed superior anti-MRSA activity compared to the control solution and other liposomes without being harmful to mammalian cells and skin. It was also observed that DA liposomes allowed Cm to reach a therapeutic intracellular level when MRSA had infected the keratinocytes.

**Table 2** Skin physiological parameters after treatment of free chloramphenicol and DA liposomes

Formulation	ΔTEWL	ΔpH	Δa*
Free drug	8.42±3.86	0.93±0.95	0.24±1.50
DA liposomes	6.24±2.30	1.32±0.66	0.27±0.74

**Notes:** ΔTEWL, the TEWL value after 7-day treatment minus the TEWL value before treatment. ΔpH, the pH value after 7-day treatment minus the pH value before treatment. Δa\*, the erythema value after 7-day treatment minus the erythema value before treatment. Each value represents the mean ± SD (n=6).

**Abbreviations:** TEWL, transepidermal water loss; DA, deoxycholic acid; SD, standard deviation.

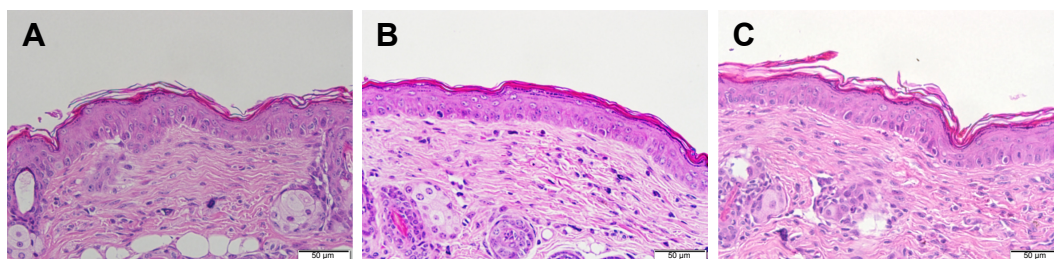


**Figure 6** Histological examination of nude mouse skin stained with H&E after 7-day treatment of topically applied control solution and DA liposomes.

Note: (A) Non-treated skin, (B) control solution, and (C) DA liposomes.  
Abbreviations: H&E, hematoxylin and eosin; DA, deoxycholic acid.

Cholesterol embedded in liposomal bilayers increases the lateral packing density, hence lowering the volume of the lipophilic phase<sup>10</sup> and resulting in the small size of classic liposomes of <100 nm. Incorporation of DMPC and DA impaired the packing density and produced larger vesicles. The deformity of DMPC and DA liposomes was confirmed by DSC. The liposomal systems provided a net negative charge, assuring physical stability due to electrostatic repulsion.<sup>23</sup>

Cm is a broad-spectrum bacteriostatic antibiotic with poor skin permeation.<sup>24</sup> Cm skin absorption and follicular uptake were improved with the flexible liposomes, especially DA containing nanocarriers. A vesicle size of <300 nm is suitable to deliver the drugs into deeper skin strata.<sup>25</sup> Our liposomes fitted this criterion. The smaller vesicles may ensure close contact with the SC and can enhance drug permeation. This was not the case in our study since the size of the malleable liposomes was much greater than that of the classic liposomes. The vesicle–skin interaction can be strongly affected by liposomal stiffness. Both SPC and cholesterol offer rigidity of liposomal bilayers.<sup>25,26</sup> DA loading into the liposomes led to crystal order imperfection and increased flexibility of the liposomal membrane. The malleable liposomes are thought to permeate facilely into the intercellular lipid bilayers, thereby enhancing drug absorption into the skin.<sup>27</sup> It is also proposed that the soft liposomes interact strongly with SC lipids,<sup>25,28</sup> creating a cutaneous reservoir for drug delivery. Follicular accumulation is generally more efficient with nanoparticles of <300 nm.<sup>29</sup> Our liposomes demonstrated an ideal size for follicular delivery. The easy transport of malleable vesicles into the appendages can be anticipated due to facile squeezing through the follicular space.<sup>7</sup>

Although DMPC liposomes showed a deformable characteristic, the skin permeation behavior of this nanocarrier was quite different from that of DA liposomes. DMPC liposomes revealed lower skin deposition but higher follicle accumulation and a greater amount of penetrated Cm in the receptor as compared with classic liposomes. The capability

of DMPC-loaded liposomes for follicular targeting has been previously reported.<sup>8</sup> Classic liposomes are of little value for topical Cm delivery as they are difficult to accumulate in the follicles compared to free Cm in alcohol/water solution. Alcohol can extract sebum in sebaceous units, making the transfollicular route predominant for drug absorption.<sup>9</sup> Due to the low resistance of the follicular epithelium, the nanocarriers diffuse quickly into the deeper strata via the follicles,<sup>30</sup> resulting in the greater Cm amount in the receptor by topical application of flexible liposomes. Easy Cm penetration into the receptor by DMPC liposomes may contribute to the limited Cm deposition remaining in the skin, although this effect was not detected with respect to DA liposomes. The follicular delivery of DMPC vesicles was less than that of DA liposomes, though the DSC profiles indicated that the DMPC system was more fluid than the DA system. The significant reduction of the melting peak and enthalpy by DMPC liposomes was attributed not only to the crystalline deficiency but also to the reduction of vesicle size. The smaller size of DMPC compared to DA liposomes led to further enthalpy decrease. It has been reported that liposomes made from DMPC are easily elongated and fluctuated.<sup>13</sup> The DMPC vesicles may be quickly disrupted in the skin because of the instability, which causes loss of benefits from the malleable feature.

It was found that DMPC incorporation raised the liposomal lipophilicity. This may be due to the long alkyl chains of DMPC increasing lipophilicity. Contrary to this result, DA had decreased liposomal lipophilicity due to the high hydrophile–lipophile balance of DA.<sup>16</sup> The follicular ducts mainly contain lipophilic material such as sebum. Lipophilic nanoparticles may exhibit a potent affinity to sebum. Our results showed no correlation between vesicle lipophilicity and follicular transport, suggesting that sebum partitioning was not the major factor predominating follicular uptake of vesicles. Elastic liposomes can keep the vesicles intact after penetrating into the lipid bilayers and follicles.<sup>10,31</sup>

For antibacterial activity, the drug should be present in a sufficient concentration at the infection site for a period of time. Cutaneous bacteria were found within the entire epidermis and appendages.<sup>4,32</sup> The epidermis and follicles can be an efficient reservoir for drug delivery. Topically applied malleable liposomes provided a possibility of sustained and targeted drug permeation in the sites of action, achieving efficient treatment and minimizing side effects.

The experimental results clearly indicated that the presence of DA in the liposomes enhanced the anti-MRSA action of Cm. The elastic vesicles have a high surface-to-volume ratio and a deformable characteristic, translating into increased interaction and fusion to bacteria and thus greater antimicrobial reaction.<sup>33,34</sup> It has been reported that the antibacterial property of nanoparticles increases following size reduction.<sup>35</sup> This was not the case in this work since DA liposomes exhibited a larger diameter than the others. Surface active nanocarriers can interact with bacteria such as *S. aureus* toward adhering and penetrating bacteria.<sup>3</sup> A low concentration of DA is found to facilely intercalate with membrane lipids of bacteria.<sup>36</sup> This DA exposure to sublethal levels allows the bacteria to adapt and protect themselves against subsequent exposure to lethal levels of DA.<sup>37</sup> This adaptation does not cause notable damage to the bacterial membrane/wall. Our results proved that DA liposomes without Cm did not display a germicidal effect. When DA liposomes directly fused with the membrane, the entrapped drug was released into the bacteria, resulting in increased contact time and a high local antimicrobial concentration. A prolonged period of antimicrobial drug treatment is always necessary to kill drug-resistant bacteria. The sustained drug release from nanoparticles provided a sufficient quantity and duration required for inhibiting bacterial growth.<sup>38</sup>

The inhibition zone treated by DA liposomes was larger than that treated by free Cm although MIC and MBC were comparable in the two groups. This may be due to the DA liposomes being able to interact with MRSA and retain an adequate drug concentration near the strain, whereas free Cm might diffuse rapidly in the agar medium. DA liposomes showed a superior anti-MRSA effect at a lower Cm concentration (0.5 mg/mL) but not at a higher concentration (1 and 2 mg/mL). The hydrophilic drugs had restricted penetration across the bacterial membrane. The hydrophilic Cm might have difficulty penetrating into the cells at a low level. As the Cm level increased, the free Cm could efficiently diffuse into the cells by the concentration gradient between the extrabacterial and intrabacterial environments. On the other hand, the

capacity of DA liposomes to adhere to bacterial membrane might be able to reach saturation at a high concentration.

Intracellular infection remains difficult to treat because of the antibiotic transport obstruction into the cytoplasm and low activity inside the host cells.<sup>39</sup> Treatment of intracellular pathogens and the subsequent spread outside the cells is an essential issue. It has been reported that the bacteria within macrophages are protected from the lethal action of Cm.<sup>40</sup> Liposomes may ensure drug passage into the cells via phospholipid bilayer-membrane fusion.<sup>14</sup> For instance, liposomal vancomycin has a marked ability to kill intracellular MRSA.<sup>41</sup> Our results indicated that Cm delivered by DA liposomes exerted significant bactericidal activity on the MRSA present within the keratinocytes. The increased cellular uptake and subsequent sustained Cm release inside the host cells effectively ameliorated the antibacterial effect. The elastic property of the DA vesicles may further promote liposomal fusion and uptake to the cells.<sup>42</sup> The entry of the DA liposomes into the mammalian cells to kill pathogens remained unclear and could not be concluded from this study. Further work is needed to clarify the mechanisms. Antimicrobial agents topically applied to treat epidermal or follicular bacteria must be able to transport into the epidermis or follicles so that they are active against intracellular and extracellular pathogens. Improved therapy of Cm entrapped in DA liposomes is expected through penetration into the skin in an intact form, followed by the facile interaction with MRSA and host cells for manifesting antibacterial efficacy.

We have shown that DA liposomes had minimal toxicity toward keratinocytes and neutrophils. Due to the intention of developing topically applied liposomes, the cytotoxicity to skin cells was inspected. Neutrophils were also examined because of the neutrophil-rich infiltration in the MRSA-infected wounds.<sup>43</sup> Neutrophils can attack MRSA to achieve infection reduction. The neutrophil viability decrease may result in the insufficient defense against MRSA. Our results demonstrated that DA liposomes did not affect this self-protection capability. According to the results of an in vivo skin irritation test, a comparable TEWL and erythema were found for the aqueous control and DA liposomes. Histology also suggested a minimal change after topical administration. No sign of skin irritation was caused by DA liposomes, though this formulation displayed a high cutaneous Cm accumulation. The materials of the elastic liposomes are mainly composed of SPC and DA, which are generally recognized as having a safe status, enabling harmless application to the skin. It is thought that topical application of the malleable

vesicles can be effective and safe for treatment of MRSA infection.

## Conclusion

It was concluded that the cutaneous delivery and anti-MRSA activity of liposomal formulations depended on the compositions. The experimental data proved that malleable liposomes facilely entered the skin reservoir and hair follicles. DA liposomes enhanced the antimicrobial properties of Cm, probably due to the increased surface area, the interaction between DA and the bacterial membrane, and sustained drug release. DA liposomes showed both extracellular and intracellular anti-MRSA activity. The results suggest that DA liposomes may be useful for the treatment of infected follicular diseases such as folliculitis, furuncle, and hidradenitis suppurativa. For good clinical implementation, further preclinical studies are required to survey the anti-MRSA effect of malleable liposomes on in vivo skin infection.

## Acknowledgment

The authors are grateful for financial support from Chang Gung Memorial Hospital (CMRPD1F0231-3 and CMRPD1D0432-3).

## Disclosure

The authors report no conflicts of interest in this work.

## References

- Martinez LR, Han G, Chako M, et al. Antimicrobial and healing efficacy of sustained release nitric oxide nanoparticles against *Staphylococcus aureus* skin infection. *J Invest Dermatol.* 2009;129:2463–2469.
- Heunis TDJ, Dicks LMT. Nanofibers offer alternative ways to the treatment of skin infections. *J Biomed Biotechnol.* 2010;2010:510682.
- Taylor E, Webster TJ. Reducing infections through nanotechnology and nanoparticles. *Int J Nanomedicine.* 2011;6:1463–1473.
- Lange-Asschenfeldt B, Marenbach D, Lang C, et al. Distribution of bacteria in the epidermal layers and hair follicles of the human skin. *Skin Pharmacol Physiol.* 2011;24:305–311.
- Laureano AC, Schwartz RA, Cohen PJ. Facial bacterial infections: folliculitis. *Clin Dermatol.* 2014;32:711–714.
- Prens E, Deckers I. Pathophysiology of hidradenitis suppurativa: an update. *J Am Acad Dermatol.* 2015;73:S8–S11.
- Fang CL, Aljuffali IA, Li YC, Fang JY. Delivery and targeting of nanoparticles into hair follicles. *Ther Deliv.* 2014;5:991–1006.
- Jung S, Otberg N, Thiede G, et al. Innovative liposomes as a transfollicular drug delivery system: penetration into porcine hair follicles. *J Invest Dermatol.* 2006;126:1728–1732.
- Tabbakhian M, Tavakoli N, Jaafari MR, Daneshamouz S. Enhancement of follicular delivery of finasteride by liposomes and niosomes 1. In vitro permeation and in vivo deposition studies using hamster flank and ear models. *Int J Pharm.* 2006;323:1–10.
- Kasetvatin C, Rujivipat S, Tiyaboonchai W. Combination of elastic liposomes and low frequency ultrasound for skin permeation enhancement of hyaluronic acid. *Colloids Surf B Biointerfaces.* 2015;135:458–464.
- Jain J, Arora S, Rajwade JM, Omray P, Khandelwal S, Paknikar KM. Silver nanoparticles in therapeutics: development of an antimicrobial gel formulation for topical use. *Mol Pharm.* 2009;6:1388–1401.
- Fang JY, Hwang TL, Huang YL, Fang CL. Enhancement of the transdermal delivery of catechins by liposomes incorporating anionic surfactants and ethanol. *Int J Pharm.* 2006;310:131–138.
- Kato N, Ishijima A, Inaba T, Nomura F, Takeda S, Takiguchi K. Effects of lipid composition and solution conditions on the mechanical properties of membrane vesicles. *Membranes.* 2015;5:22–47.
- Xie S, Tao Y, Pan Y, et al. Biodegradable nanoparticles for intracellular delivery of antimicrobial agents. *J Control Release.* 2014;187:101–117.
- Lee WR, Shen SC, Sun CK, et al. Fractional thermolysis by bipolar radiofrequency facilitates cutaneous delivery of peptide and siRNA with minor loss of barrier function. *Pharm Res.* 2015;32:1704–1713.
- Lee WR, Shen SC, Aljuffali IA, Li YC, Fang JY. Erbium-yttrium-aluminum-garnet laser irradiation ameliorates skin permeation and the follicular delivery of antialopecia drugs. *J Pharm Sci.* 2014;103:3542–3552.
- Hoopman TC, Liu W, Joslin SN, Pybus C, Brautigam CA, Hansen EJ. Identification of gene products involved in the oxidative stress response of *Moraxella catarrhalis*. *Infect Immun.* 2011;79:745–755.
- Mu H, Tang J, Liu Q, Sun C, Wang T, Duan J. Potent antibacterial nanoparticles against biofilm and intracellular bacteria. *Sci Rep.* 2016;6:18877.
- Richardson AR, Libby SJ, Fang FC. A nitric oxide-inducible lactate dehydrogenase enables *Staphylococcus aureus* to resist innate immunity. *Science.* 2008;319:1672–1676.
- Johnson MB, Criss AK. Fluorescence microscopy methods for determining the viability of bacteria in association with mammalian cells. *J Vis Exp.* 2013;79:e50729.
- Pan TL, Wang PW, Aljuffali IA, Huang CT, Lee CW, Fang JY. The impact of urban particulate pollution on skin barrier function and the subsequent drug absorption. *J Dermatol Sci.* 2015;78:51–60.
- Hwang TL, Sung CT, Aljuffali IA, Chang YT, Fang JY. Cationic surfactants in the form of nanoparticles and micelles elicit different human neutrophil responses: a toxicological study. *Colloids Surf B Biointerfaces.* 2014;114:334–341.
- Sandri G, Bonferoni MC, D’Autilia F, et al. Wound dressings based on silver sulfadiazine solid lipid nanoparticles for tissue repairing. *Eur J Pharm Biopharm.* 2013;84:84–90.
- Kalita S, Devi B, Kandimalla R, et al. Chloramphenicol encapsulated in poly-ε-caprolactone-pluronic composite: nanoparticles for treatment of MRSA-infected burn wounds. *Int J Nanomedicine.* 2015;10:2971–2984.
- Verma P, Pathak K. Nanosized ethanolic vesicles loaded with econazole nitrate for the treatment of deep fungal infections through topical gel formulation. *Nanomedicine.* 2012;8:489–496.
- Corvera E, Mouritsen OG, Singer MA, Zuckermann MJ. The permeability and the effect of acyl-chain length for phospholipid bilayers containing cholesterol: theory and experiment. *Biochim Biophys Acta.* 1992;1107:261–270.
- Elmoslemany RM, Abdallah OY, El-Khordagui LK, Khalafallah NM. Propylene glycol liposomes as a topical delivery system for miconazole nitrate: comparison with conventional liposomes. *AAPS PharmSciTech.* 2012;13:723–731.
- Manconi M, Mura S, Sinico C, Fadda AM, Vila AO, Molina F. Development and characterization of liposomes containing glycols as carriers for diclofenac. *Colloids Surf A.* 2009;342:53–58.
- Morgen M, Lu GW, Du D, et al. Targeted delivery of a poorly water-soluble compound to hair follicles using polymeric nanoparticle suspensions. *Int J Pharm.* 2011;416:314–322.
- Aljuffali IA, Pan TL, Sung CT, Chang SH, Fang JY. Anti-PDGF receptor β antibody-conjugated squarticles loaded with minoxidil for alopecia treatment by targeting hair follicles and dermal papilla cells. *Nanomedicine.* 2015;11:1321–1330.

31. Subongkot T, Wonglertnirant N, Songprakhon P, Rojanarata T, Opanasopit P, Ngawhirunpat T. Visualization of ultradeformable liposomes penetration pathways and their skin interaction by confocal laser scanning microscopy. *Int J Pharm.* 2013;442:151–161.
32. Grice EA, Segre JA. The skin microbiome. *Nat Rev Microbiol.* 2011;9:244–253.
33. Hadinoto K, Cheow WS. Nano-antibiotics in chronic lung infection therapy against *Pseudomonas aeruginosa*. *Colloids Surf B Biointerfaces.* 2014;116:772–785.
34. Aljuffali IA, Huang CH, Fang JY. Nanomedical strategies for targeting skin microbiomes. *Curr Drug Metab.* 2015;16:255–271.
35. Panacek A, Kvitek L, Prucek R, et al. Silver colloid nanoparticles: synthesis, characterization, and their antibacterial activity. *J Phys Chem B.* 2006;110:16248–16253.
36. Begley M, Gahan CGM, Hill C. The interaction between bacteria and bile. *FEMS Microbiol Rev.* 2005;29:625–651.
37. O'Driscoll B, Gahan CGM, Hill C. Adaptive acid tolerance response in *Listeria monocytogenes*: isolation of an acid-tolerant mutant which demonstrates increased virulence. *Appl Environ Microbiol.* 1996;62:1693–1698.
38. Kalhapure RS, Sonawane SJ, Sikwal DR, et al. Solid lipid nanoparticles of clotrimazole silver complex: an efficient nano antibacterial against *Staphylococcus aureus* and MRSA. *Colloids Surf B Biointerfaces.* 2015;136:651–658.
39. Zazo H, Colino CI, Lanao JM. Current applications of nanoparticles in infectious diseases. *J Control Release.* 2016;224:86–102.
40. Kiruthika V, Maya S, Suresh MK, Kumar VA, Jayakumar R, Biswas R. Comparative efficacy of chloramphenicol loaded chondroitin sulfate and dextran sulfate nanoparticles to treat intracellular *Salmonella* infections. *Colloids Surf B Biointerfaces.* 2015;127:33–40.
41. Zhang L, Pornpattananangkul D, Hu CMJ, Huang CM. Development of nanoparticles for antimicrobial drug delivery. *Curr Med Chem.* 2010;17:585–594.
42. Wen CJ, Sung CT, Aljuffali IA, Huang YJ, Fang JY. Nanocomposite liposomes containing quantum dots and anticancer drugs for bioimaging and therapeutic delivery: a comparison of cationic, PEGylated, and deformable liposomes. *Nanotechnology.* 2013;24:325101.
43. Kinoshita M, Miyazaki H, Ono S, et al. Enhancement of neutrophil function by interleukin-18 therapy protects burn-injured mice from methicillin-resistant *Staphylococcus aureus*. *Infect Immun.* 2011;79:2670–2680.

International Journal of Nanomedicine

## Publish your work in this journal

The International Journal of Nanomedicine is an international, peer-reviewed journal focusing on the application of nanotechnology in diagnostics, therapeutics, and drug delivery systems throughout the biomedical field. This journal is indexed on PubMed Central, MedLine, CAS, SciSearch®, Current Contents®/Clinical Medicine,

Submit your manuscript here: <http://www.dovepress.com/international-journal-of-nanomedicine-journal>

Dovepress

Journal Citation Reports/Science Edition, EMBase, Scopus and the Elsevier Bibliographic databases. The manuscript management system is completely online and includes a very quick and fair peer-review system, which is all easy to use. Visit <http://www.dovepress.com/testimonials.php> to read real quotes from published authors.